

Published in final edited form as:

*Health Phys.* 2013 May ; 104(5): 471–480. doi:10.1097/HP.0b013e318284f461.

## SHIELDING CONSIDERATIONS FOR THE SMALL ANIMAL RADIATION RESEARCH PLATFORM (SARRP)

Elaine Sayler, Derek Dolney, Stephen Avery, and Cameron Koch\*

\*Department of Radiation Oncology, University of Pennsylvania, John Morgan Building, 3620 Hamilton Walk, Philadelphia, PA 19104

### Abstract

The Small Animal Radiation Research Platform (SARRP) is a commercially available platform designed to deliver conformal, image-guided radiation to small animals using a dual-anode kV x-ray source. At the University of Pennsylvania, a free-standing 2 m<sup>3</sup> enclosure was designed to shield the SARRP according to federal code regulating cabinet x-ray systems. The initial design consisted of 4.0-mm-thick lead for all secondary barriers and proved wholly inadequate. Radiation levels outside the enclosure were 15 times higher than expected. Additionally, the leakage appeared to be distributed broadly within the enclosure, so concern arose that a subject might receive significant doses outside the intended treatment field. Thus, a detailed analysis was undertaken to identify and block all sources of leakage. Leakage sources were identified by Kodak X-OmatV (XV) film placed throughout the enclosure. Radiation inside the enclosure was quantified using Gafchromic film. Outside the enclosure, radiation was measured using a survey meter. Sources of leakage included (1) an unnecessarily broad beam exiting the tube, (2) failure of the secondary collimator to confine the primary beam entirely, (3) scatter from the secondary collimator, (4) lack of beam-stop below the treatment volume, and (5) incomplete shielding of the x-ray tube. The exit window was restricted, and a new collimator was designed to address problems (1–3). A beam-stop and additional tube shielding were installed. These modifications reduced internal scatter by more than 100-fold. Radiation outside the enclosure was reduced to levels compliant with federal regulations, provided the SARRP is operated using tube potentials of 175 kV or less. In addition, these simple and relatively inexpensive modifications eliminate the possibility of exposing a larger animal (such as a rat) to significant doses outside the treatment field.

### Keywords

laboratory animals; radiation protection; radiobiology; shielding; small animal radiation research platform

## INTRODUCTION

The small Animal Radiation Research Platform (SARRP) is a commercially available image-guided microirradiation system produced by Xstrahl [Gulmay Medical Inc. (an Xstrahl Ltd. company), 480 Brodgon Rd., Suwanee, GA USA]. The platform includes a robotic stage with four degrees of freedom for positioning animals. A Varian model NDI-225-22 kV x-ray tube is mounted on a gantry that rotates between 0–120 degrees. The power source for the x-ray tube operates under constant voltage (1–225 kV) and current (0.1–15 mA). Cone beam computed tomography (CBCT) images can be acquired by rotating the animal between the (horizontal) x-ray source and a stationary flat-panel detector. The x-ray source has a dual anode: a small focal spot is used at low power for imaging, and a large focal spot is used at high power for therapy. The CBCT requires a wide-field beam, whereas the therapeutic beam must be highly collimated. These contrasting requirements require a versatile collimation system (Wong et al. 2008).

The SARRP collimating system is shown in Fig. 1. Upon exiting the x-ray tube window, the beam is shaped by a brass primary collimator. A secondary collimator, consisting of a wide base and a long nozzle, affixes to the primary collimator and produces an open field roughly 12 mm in diameter. Interchangeable tertiary collimators attach to the nozzle to change the field size. The standard therapeutic field sizes range from  $0.5 \times 0.5 \text{ mm}^2$  to  $5 \times 5 \text{ mm}^2$  (Wong et al. 2008; Deng et al. 2007). These features allow for highly conformal treatments, making SARRP a powerful tool in translational research (Ford et al. 2011; Armour et al. 2010; Ngwa et al. 2011).

In the interest of safety and compliance with federal regulations, prospective SARRP users will want to prepare the necessary shielding before delivery of the platform. SARRP users will want to ensure that radiation levels are below the annual dose limits of 50 mSv to radiation workers and 5 mSv to the public (USNRC 2012). In addition, for a cabinet-type enclosure, the exposure at 5 cm from the shielded surface must be below  $0.129 \mu\text{C kg}^{-1}$  (0.5 mR) in any 1 h (USFDA 2012).

The manufacturer recommends that the SARRP be installed in a radiation-controlled area within a shielded room.<sup>†</sup> However, such a room may not be available or practical in many laboratories. This was the authors' situation, so a free-standing enclosure was designed to shield the SARRP. This report describes experiences achieving acceptable radiation levels outside of the enclosure, which was accomplished primarily through modifications of the SARRP itself.

## METHODS

The SARRP enclosure (Fig. 2) was constructed of lead sheets mounted to plywood and supported by axn aluminum frame. A door with a leaded glass window allows access to the SARRP. The enclosure was installed with minimum shielding (4.0-mm-thick lead) with the option to increase the thickness. The authors predicted that 4.0 mm of lead would be

---

<sup>†</sup>Gulmay Medical Ltd. SARRP image guided microirradiation technical description. March 2010 (unpublished).

sufficient based on shielding calculations and the assumption that radiation outside the primary beam would be low-energy scatter.

After installation of the SARRP and its enclosure, a preliminary survey revealed that radiation levels outside the enclosure were much higher than anticipated. An initial film survey showed that radiation levels inside the enclosure (but outside the treatment field) were also much higher than anticipated. Thus concern arose that an animal might be exposed to significant doses outside the planned treatment field. The approach to solve both problems was to block the out-of-field radiation as far upstream (i.e., close to the radiation source) as practical. This strategy ensures protection of the animal outside the treatment field and also reduced the need for additional lead shielding.

Five significant sources of leakage radiation were identified: (1) an unnecessarily broad beam exiting the tube (i.e., much greater than necessary to cover the flat-panel detector of the CBCT), (2) failure of the secondary collimator to arrest the primary beam, (3) scatter from the secondary and tertiary collimator, (4) incomplete shielding of the x-ray tube, and (5) lack of beam-block below the target.

### Exit window

The primary beam exits the beryllium window with a square cross section and spreads at an angle of roughly 20 degrees from vertical. To visualize this, a block was fabricated from Corian plastic (E.I. du Pont de Nemours and Company, 1007 N. Market St., Wilmington, DE USA Wilmington, DE) with dimensions of  $96 \times 68 \times 12 \text{ mm}^3$ , which is the exact size of the rectangular base of the standard SARRP secondary collimator. Corian is a strong and stable polymer that is easy to machine and has the unexpected but useful property that, when exposed to radiation, it changes color from white to violet in a dose-dependent manner. The Corian block was inserted into the collimator tray (as the secondary collimator would be) and the x-ray was turned on. The resulting color change in the Corian indicated two important problems: (1) The solid angle of the primary beam was much greater than necessary to fully cover the flat panel detector, and (2) the rectangular stainless steel base of the collimator did not extend far enough back (toward the cathode of the x-ray tube) to block the primary beam.

As a consequence of the exit window and secondary collimator design, a significant portion of the primary beam was blocked by only 12 mm of stainless steel (the thickness of the standard collimator base), and a small fraction of the beam was essentially unblocked. To address problem (1) a cylindrical lead sleeve (height = 23 mm, outer diameter = 38 mm, wall thickness = 5 mm) was inserted inside the exit window above the primary collimator. This constrained the tube output to a circular field with a diameter just large enough to cover the flat panel detector (Fig. 3).

### Secondary collimation

To address problem (2), the thin brass bar that formed the backstop of the collimator tray was removed and replaced with two washers (Fig. 3). This opened the ear of the collimator tray, allowing an extension of the Corian block or collimator base. A wider Corian block, extending past the brass washers, was fabricated with dimensions of  $96 \times 88 \times 25 \text{ mm}^3$ . In

conjunction with the restricted window size, the larger block was found to contain the primary beam completely. At this point, a new secondary collimator was fabricated in-house. The base of the new collimator is solid brass, with dimensions  $96 \times 88 \times 25 \text{ mm}^3$ . The standard collimator base is a steel alloy with dimensions  $96 \times 66 \times 12 \text{ mm}^3$  (Fig. 4).

### **Collimator scatter**

The standard secondary collimator features an open, aluminum alloy nozzle. Radiation escapes from the open portion of the nozzle and also scatters from the junction between the aluminum nozzle and the brass tertiary collimator. In this redesign of the collimator, both sources of collimator scatter were blocked by using a solid brass nozzle (Fig. 4). The interchangeable tertiary collimators fit into both nozzles.

### **Tube leakage**

Once the primary beam was fully blocked it became apparent that the x-ray tube itself was not completely shielded. A narrow beam of high-energy photons was penetrating the anode end of the x-ray tube, and diffuse radiation was leaking from the sides. The leakage radiation can be eliminated by installing a 3.2-mm-thick piece of lead at the end of the tube and a U-shaped piece around the body.

### **Scatter from robotic stage**

Scattered radiation from the robotic stage was also observed. The scatter becomes more pronounced at the larger field sizes and likely arises from Compton scattering of photons in the aluminum. A 3.2-mm-thick lead beam stop was installed on top of the robotic stage.

It was confirmed that these modifications to the SARRP effectively blocked sources of leakage radiation by exposing Kodak X-Omat V (XV) Films (Carestream Health Inc., 150 Verona St., Rochester, NY USA) at different locations inside the enclosure before and after each of the five modifications described above.

To quantify the leakage radiation, the dose rates at specific points of interest were measured before and after modifications using Gafchromic EBT2 film (Ashland Inc., 50 E. River Center Blvd., Covington, KY USA). The Gafchromic film was calibrated in the SARRP against an ion chamber, as described by Tryggestad et al. (2009). The film was scanned using an ArtixScan M1 film scanner (Microtek International Inc., 9960 Bell Ranch Dr., Santa Fe Springs, CA USA). This dosimetry protocol uses in-house Matlab (The MathWorks Inc., 3 Apple Hill Dr., Natick, MA USA) code to analyze the red channel, as described by Devic et al. (2005).

Lastly, a radiation survey was completed outside the glass window of the enclosure before and after each modification using an Ion Chamber Survey Meter, Model 9-3 (Ludlum Measurements Inc., 405 Oak St., Sweetwater, TX USA).

### **Treatment energy**

To achieve an exposure rate of less than  $0.129 \mu\text{C kg}^{-1} \text{ h}^{-1}$  at 5 cm from the surface of the enclosure, the SARRP was commissioned at 175 kV instead of the SARRP standard of 220

kV. At 225 kV, the tenth value layer (TVL) is 2.3 mm of lead, while at 175 kV the TVL is only 1.3 mm of lead (NCRP 1976). By simply lowering the treatment energy, identical shielding provided exponentially more radiation protection.

The effects of changing the treatment energy call for careful consideration with regard to dosimetry. Currently, the SARRP treatment planning system does not correct for tissue heterogeneities. Users must be aware that at kV energies, the photoelectric effect causes significantly more dose to be deposited in bone than in tissue. When treating at 225 kV, roughly 3.9 times more dose is deposited in bone than in tissue. However, when treating at 175 kV, bone absorbs a dose 4.5 times greater than tissue (Table 1) (Hubbel and Selzer 2004). Thus, delivering a given dose to tissue with the lower energy can result in a 15% higher dose to bone, and users should carefully consider the implications for their experiments.

### **Shielded capsule design**

To evaluate the efficacy of the shielded enclosure, the entire enclosure was covered with XV film. The film envelopes were numbered, and features of the capsule were traced onto the envelopes. Upon development, exposure on each film was identified and registered to a physical feature on the capsule. Thus any points of weakness in the enclosure were identified.

## **RESULTS**

### **Corian beam block study**

The Corian block illustrates that the lead sleeve restricts the beam path effectively. After being exposed in the collimator tray, the Corian block (with dimensions identical to the standard collimator) turned violet along the beam's path (Fig. 5). A view of the rear (cathode) side of the block reveals that the beam path diverges out of the block. The original (square) beam path is highlighted with a dashed line, and the restricted (circular) beam path is highlighted with a solid line. It is clear that the lead sleeve reduces the area of beam diverging past the block significantly. It is also clear that a wider block is necessary to contain the beam fully.

The larger block (with dimensions identical to the modified collimator) demonstrates that a larger collimator base, in conjunction with the restricted exit window, fully attenuates the primary beam. Fig. 6 shows the exposure on the top and bottom of the larger Corian blocks with and without the lead sleeve restricting the size of the exit window. The field incident on the block extends exactly to the edge of the original collimator footprint. Without widening the base of the collimator, a portion of the primary beam passes the edge of the collimator unattenuated.

### **XV film study**

The XV films shown in Fig. 7 were exposed while lying flat on the specimen stage (A) before any modifications, (B) after installation of the cylindrical lead sleeve in the x-ray tube exit window, and (C) with the modified secondary collimator. In the center of all films, the

intended treatment field is visible. The portion of the beam directly outside the intended treatment field is attenuated by the near-circular brass portion of the standard collimator. However, with the standard (square) exit window (A), the beam outside a roughly 10-cm radius of the treatment field is attenuated only by the rectangular stainless steel collimator base. It is clear that this is not sufficient. By restricting the size of the exit window (B), the beam is mostly contained by the brass portion of the standard collimator. The modified collimator (C), with its wider and thicker brass base, fully contains the primary beam outside the intended treatment field. The solid brass nozzle eliminates scatter from the open nozzle design and from the junction between the aluminum nozzle of the secondary collimator and the brass tertiary collimator (Fig. 4).

The XV films compared in Fig. 8 were exposed 15 cm behind the nozzle, in the plane of gantry rotation, with the (A) standard and (B) modified collimator. The lead sleeve was inserted in the exit window for both exposures. In the film exposed with the standard collimator (A), the most superior area of exposure is due to radiation scattered from the steel collimator base. The exposure in the lower portion of the film corresponds to the area of high exposure seen in Fig. 7b and is a result of the standard secondary collimator base failing to confine the primary beam entirely. The new collimator's wider and thicker brass base eliminates both of these sources of radiation.

The XV films compared in Fig. 9 demonstrate the inadequate shielding of the x-ray tube. The films were taped 3 cm in front of (i.e., the anode side of) the x-ray tube and exposed (A) without the lead tube block and (B) with the tube block. The film exposed without the tube block (A) exhibits darkening on the film corresponding to the location of the source, suggesting that some high-energy photons penetrate the anode and the tube housing. The point source is not evident in the film exposed with the tube block in place (B), demonstrating that 3.2 mm of lead is sufficient to shield this leakage radiation.

The XV films shown in Fig. 10 demonstrate that the beam stop reduces scatter modestly from the robotic stage. The features of the robotic stage are discernible from scattered radiation in the film exposure without the beam stop (A). There is no scatter from the stage evident on the film exposed with the beam stop (B). The effect of the beam stop becomes more pronounced as larger field sizes, or an open field, are used.

Lastly, the XV film exposed on the outside of the SARRP enclosure revealed two major weaknesses. First, some radiation was escaping through the crack between the door and the doorframe, despite a lead radiation baffle. This leakage was blocked by widening the baffle from 3 cm to 10 cm. This issue suggests that for shielding purposes, SARRP should be considered a broad source. This is further supported by the internal films, which illustrate multiple scattering sites. Secondly, the attenuation provided by the leaded glass window was much less than calculated, based on the "lead equivalence" specified by the manufacturer. This underestimate was rectified by using 4.8-mm-thick lead equivalent glass plus an additional 24.5-mm plate glass. The authors would recommend that future SARRP users consider a smaller window, placed where tube leakage and target scatter will be minimal.

### Film dosimetry study

The lead sleeve and modified collimator reduce radiation significantly outside the treatment field. The dose rate inside and outside the treatment field was measured using Gafchromic film. Table 2 lists the percent of the treatment dose received outside the treatment field (in the area of highest exposure, apparent in Fig. 7) for different field sizes, with and without the sleeve inserted, with the standard versus modified collimator. Without the lead sleeve, the maximum dose rate outside the field (in the apparent area of highest exposure) was approximately  $15 \text{ cGy min}^{-1}$  at 35 cm source-to-surface distance (SSD) for all field sizes. With the sleeve inserted, the maximum dose rate was approximately  $3 \text{ cGy min}^{-1}$ , and the modified collimator further reduced it to a roughly uniform  $1 \text{ cGy min}^{-1}$ . The percent of treatment dose received outside the treatment field is different for each field size, as each tertiary collimator has a slightly different output.

### Radiation survey

The modifications to the SARRP significantly reduced the radiation levels outside the enclosure with no major changes to the enclosure itself. Table 3 illustrates the reduction in exposure rate for the modifications to the collimator assembly. Table 4 shows the reduction in exposure rate from use of a beam stop, a tube block, and lower treatment energy. The measurements were taken at different locations on the surface of the glass window, which corresponds roughly to 45 cm off-axis. These modifications reduce the radiation to well below acceptable levels.

## DISCUSSION

The most significant reduction in leakage radiation was achieved by blocking the scatter and leakage around the collimator assembly. The redesigned collimator assembly eliminates the possibility of delivering up to 9% of the treatment dose outside the treatment field, irrespective of external shielding design. These modifications are particularly important for a lab considering experiments that involve treating multiple animals in a single setup or labs considering housing animals inside the SARRP shielding.

This analysis of radiation outside of the treatment volume dealt primarily with the standard small fields. However, normal use of SARRP might frequently require large fields. For example, daily output checks are performed with an open field (i.e., no secondary or tertiary collimator). This lab has also seen a demand for large (12-cm-diameter) treatment fields. A large field poses additional shielding challenges. The output is obviously much higher, and scattered radiation from the primary beam becomes a more significant problem. Additionally, the primary beam can diverge at up to a 20-degree angle from vertical; if the shielded enclosure is not designed properly, the primary beam could impinge on the external barrier (e.g., a side of the enclosure). A simple solution is to use a large beam stop during any large or open-field exposures. A lead beam stop is also a good solution to prevent the primary beam from being scattered by the aluminum robotic stage.

After the physical modifications to the SARRP, the maximum exposure rate at the surface of the SARRP enclosure, while treating at 225 kV, was  $0.52 \text{ } \mu\text{C kg}^{-1} \text{ h}^{-1}$ . Given the relatively

low workload of the SARRP (5 h wk<sup>-1</sup> treatment, 5 h wk<sup>-1</sup> imaging at 65 kV), the SARRP boratory is well under the maximum annual occupational dose limit of 50 mSv y<sup>-1</sup> (USNRC 2012). Under normal operating conditions, this SARRP does not have more than 15 min of “beam on” time in any 1 h. Thus the SARRP is also in compliance with the FDA exposure limit for cabinet x-rays of 0.129  $\mu\text{C kg}^{-1}$  in any 1 h (USFDA 2012). However, in this lab, a conservative approach was taken and limited the treatment energy to 175 kV in order to reduce the *instantaneous* exposure rate to below 0.129  $\mu\text{C kg}^{-1} \text{ h}^{-1}$ . Treating with an open field at 175 kV, the exposure rate at all surfaces of the enclosure is less than 0.129  $\mu\text{C kg}^{-1} \text{ h}^{-1}$ .

Additionally, the maximum exposure rate was measured consistently at the surface of the glass window. Outside the lead surfaces of the enclosure, the exposure rate was measured to be less than 0.03  $\mu\text{C kg}^{-1} \text{ h}^{-1}$  while treating at 225 kV. If a SARRP user wanted to shield SARRP as a cabinet-type x-ray unit, it would be possible to use a version of this enclosure that either did not include a leaded glass window or used a thicker leaded glass barrier. The authors speculate that the “lead equivalence” of the glass specified by the manufacturer is for rectified AC machines and is not correct for the energy spectrum produced by a tube driven with a constant voltage source.

## CONCLUSION

Shielding the SARRP in an in-house designed, cabinet-type enclosure may not be the approach for most users and indeed is not recommended by the manufacturer. However, in doing so, the authors have identified sources of leakage that expose the subject to unnecessarily high scattered radiation. They have identified several simple and inexpensive solutions to reduce the excess radiation. These improvements also reduce the leakage through the enclosure to below levels required by federal regulations.

Other SARRP users may want to consider these modifications to the collimator system. The design of the existing collimator could in fact expose a larger animal (such as a rat) to significant doses outside the treatment field. For instance, if the flank was being treated but the animal’s head was facing in the cathode direction, it could receive significant dose to the head. Narrowing the x-ray window, enlarging the secondary collimator base, and using a closed tube have no adverse effects on the use of SARRP.

The tube block, lead sleeve, modified secondary collimator, and beam stop significantly reduce the amount of shielding necessary for SARRP. For laboratories without a designated shielded room, these small changes reduce shielding requirements dramatically. In addition, lowering the beam’s energy by 50 kV (from 225 kV to 175 kV) reduces the necessary amount of shielding without significantly affecting the depth-dose characteristics of the beam in water (though the bone dose will be higher for a given tissue dose).

Prospective SARRP users should consider carefully the design of doors and windows on a shielded enclosure. For shielding purposes, the SARRP should be considered a broad source. Windows should be as small as practical, and their thickness should be determined using a conservative estimate, because nearly all leakage from the enclosure escaped through the

window (4.8-mm lead-equivalent glass plus 24.5-mm plate glass) rather than through the actual lead panels (2.4-mm lead). The authors believe that a radiologically thicker glass window would provide enough shielding to operate SARRP at 225 kV in compliance with FDA regulations.

## Acknowledgments

Special thanks to Tim Jenkins, Chris Kennedy, and James Weltz for their contributions to the SARRP project at the University of Pennsylvania. Bob Lukasik provided technical support from Gulmay Medical Ltd. Funding for the SARRP was provided by NCI equipment grant 1S10RR026587-01.

## References

- Armour M, Ford E, Iordachita I, Wong J. CT guidance is needed to achieve reproducible positioning of the mouse head for repeat precision cranial irradiation. *Radiat Res.* 2010; 173:119–123. [PubMed: 20041766]
- Deng H, Kennedy CW, Armour E, Tryggestad E, Ford E, McNutt T, Jiang L, Wong J. The small-animal radiation research platform (SARRP): dosimetry of a focused lens system. *Phys Med Biol.* 2007; 52:2729–2740. [PubMed: 17473348]
- Devic S, Seuntjens J, Sham E, Podgorsak EB, Schmidtlein CR, Kirov AS, Soares CG. Precise radiochromic film dosimetry using a flat-bed document scanner. *Med Phys.* 2005; 32:2245–2253. [PubMed: 16121579]
- Ford EC, Achanta P, Purger D, Armour M, Reyes J, Fong J, Kleinberg L, Redmond K, Wong J, Jang MH, Jun H, Song HJ, Quinones-Hinojosa A. Localized CT-guided irradiation inhibits neurogenesis in specific regions of the adult mouse brain. *Radiat Res.* 2011; 175:774–783. [PubMed: 21449714]
- Hubbell, JH.; Seltzer, SM. Tables of x-ray mass attenuation coefficients and mass energy-absorption coefficients (version 1.4). Gaithersburg, MD: National Institute of Standards and Technology; 2004. Available at <http://physics.nist.gov/xaamdi>. Accessed 20 1 2012
- National Council of Radiation Protection and Measurements. Structural shielding design and evaluation for medical use of x rays and gamma rays of energies up to 10 MeV. Washington DC: NCRP Publications; 1976. NCRP Report No. 49[third reprinting 1998]
- Ngwa W, Korideck H, Chin LM, Makrigiorgos GM, Berbeco RI. MOSFET assessment of radiation dose delivered to mice using the Small Animal Radiation Research Platform (SARRP). *Radiat Res.* 2011; 176:816–820. [PubMed: 21962005]
- Tryggestad E, Armour M, Iordachita I, Verhaegen F, Wong JW. A comprehensive system for dosimetric commissioning and Monte Carlo validation for the small animal radiation research platform. *Phys Med Biol.* 2009; 54:5341–5357. [PubMed: 19687532]
- U.S. Food and Drug Administration. Performance standards for ionizing radiation emitting products. Washington, DC: U.S. Government Printing Office; 2012. 21 CFR Part 1020.40
- U.S. Nuclear Regulator Commission. Standards for protection against radiation. Washington, DC: U.S. Government Printing Office; 2012. 10DFR Part 20
- Wong J, Armour E, Kazanzides P, Iordachita I, Tryggestad E, Hua D, Matinfar M, Kennedy C, Liu Z, Chan T, Gray O, Verhaegen F, McNutt T, Ford E, DeWeese TL. A high resolution small animal radiation research platform (SARRP) with x-ray tomographic guidance capabilities. *International J Radiat Oncol Biol Phys.* 2008; 71:1591–1599.

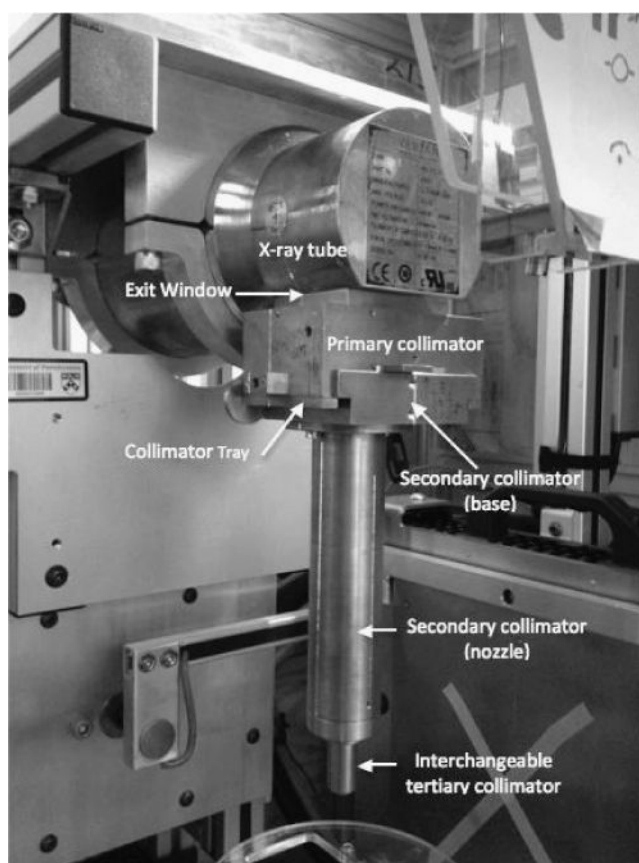


**Fig. 1.**  
SARRP collimating system.



**Fig. 2.**

SARRP Laboratory at University of Pennsylvania: The SARRP enclosure is roughly  $1.8 \times 2.1 \times 2.1 \text{ m}^3$ , constructed of 4.0-mm-thick lead walls and a  $0.9 \times 1.2 \text{ m}^2$  door that includes a  $0.6 \times 0.9 \text{ m}^2$  window with 4.8-mm-thick lead equivalent plus 25.4-mm plate glass.

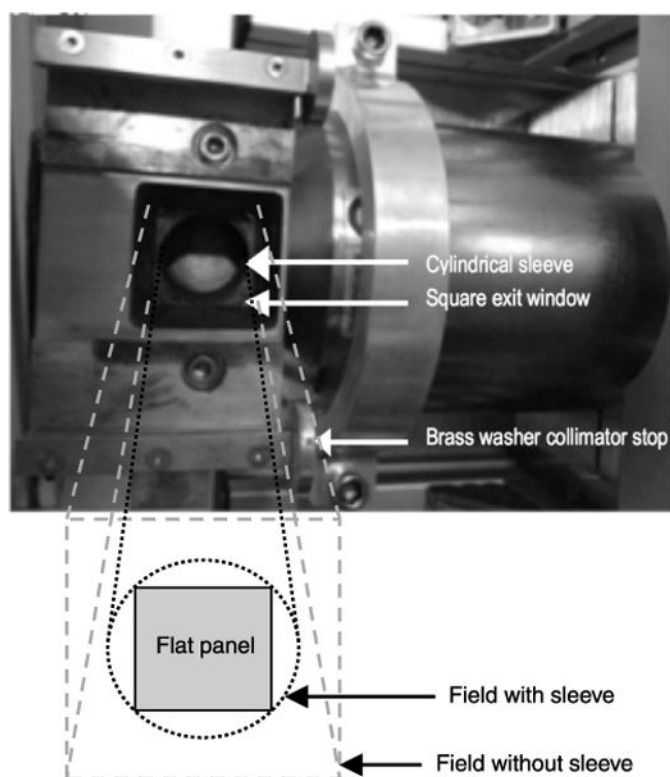


**Fig. 3.**

View (into x-ray tube window) of modifications to the exit window and secondary collimator tray, with illustration of beam geometry. A cylindrical lead sleeve restricts the size of the exit window such that the beam is just large enough to cover the flat panel detector. The collimator tray backstop has been replaced with two brass washers, allowing insertion of a larger collimator. (Illustration of beam geometry is not to scale.)

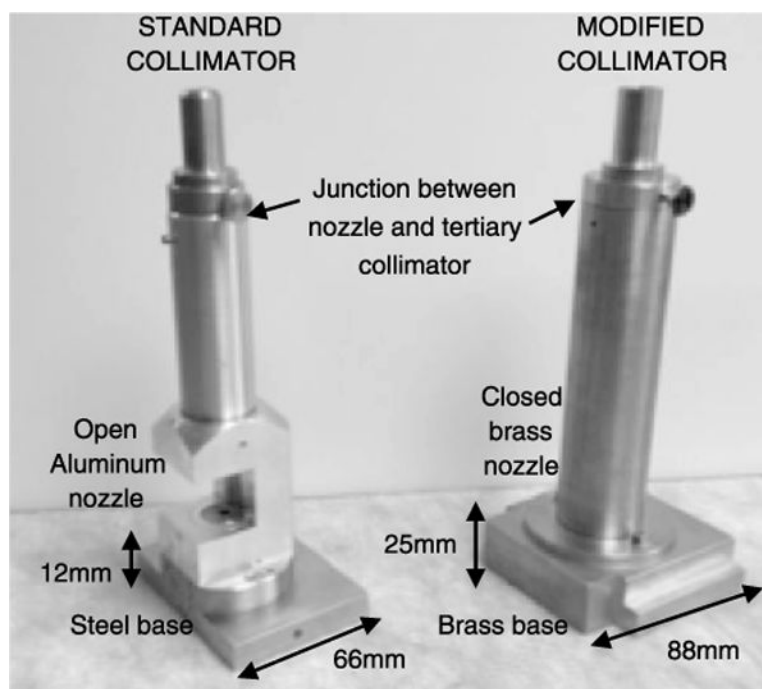


**Fig. 4.** Standard and modified collimators: The new collimator features a wider, thicker brass base to fully block the primary beam, and a solid brass tube to reduce collimator scatter.

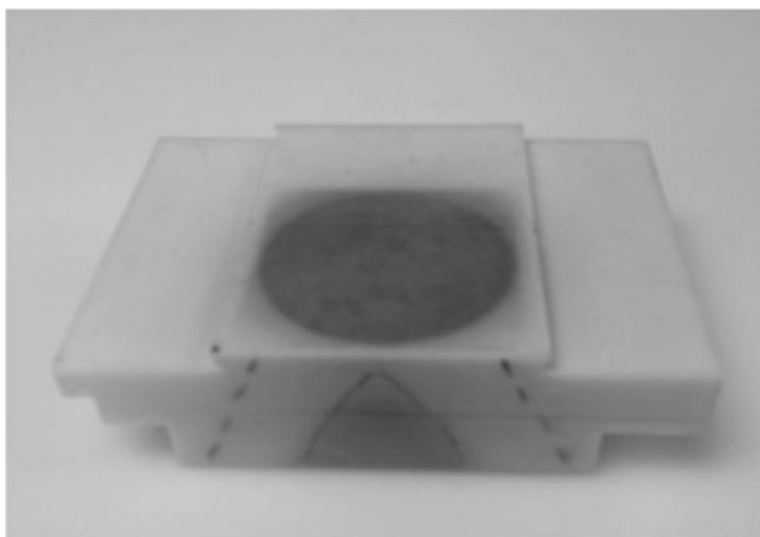


**Fig. 5.** Rear view of Corian block (standard footprint) after exposure: Darkening of the Corian illustrates the beam path with (solid line) and without (dashed line) the cylindrical sleeve. While both beams diverge out of the back of the beam block, the cylindrical sleeve reduces the portion of the beam that is inadequately attenuated by the standard collimator.

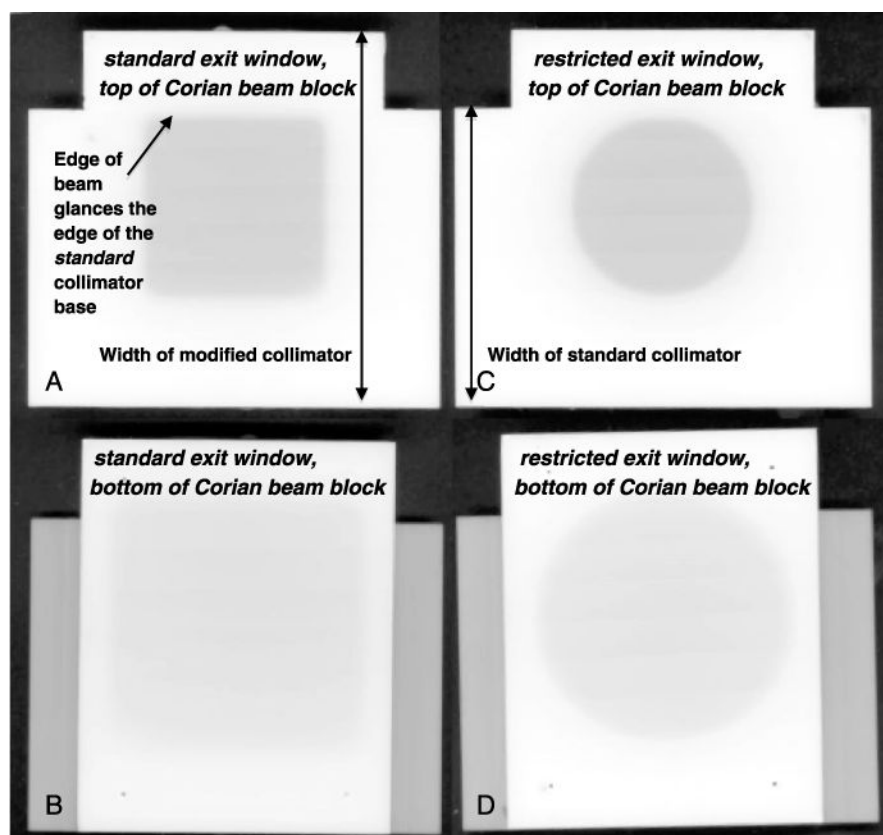


**Fig. 6.** Corian blocks with dimensions identical to the modified (larger) collimator base after exposure in collimator tray, comparing beams from the (A,B) standard and (C,D) restricted exit windows. The combination of enlarging the collimator base and restricting the exit window size completely blocks the primary beam.

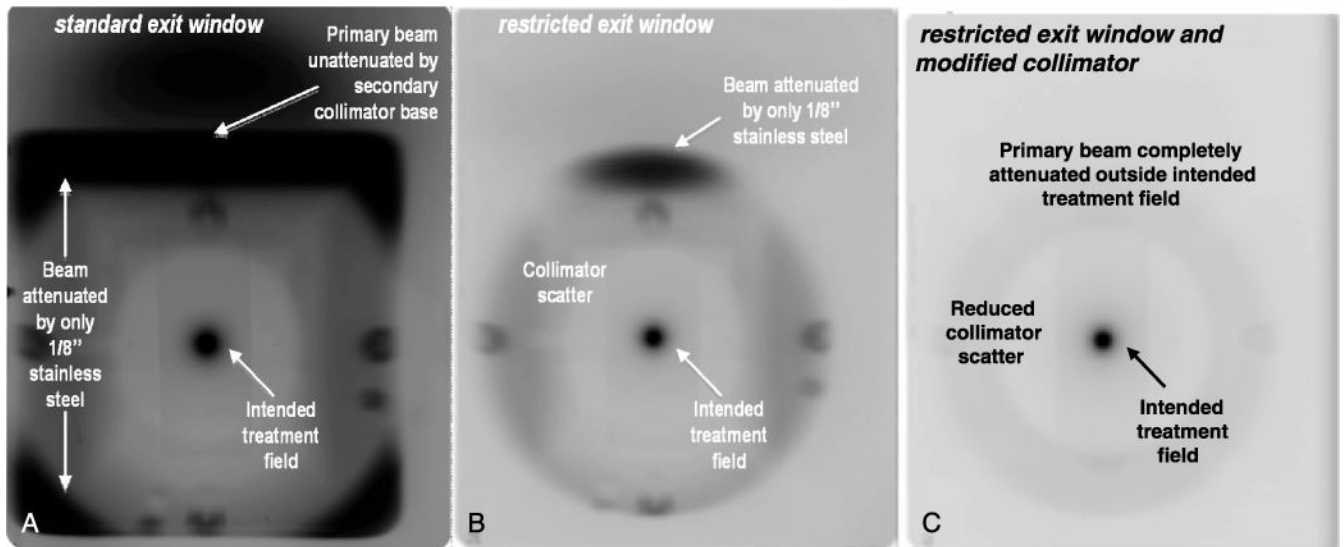


**Fig. 7.**

XV films comparing radiation in the plane of a  $5 \times 5 \text{ mm}^2$  treatment field (35 cm SSD) with (A) standard exit window and standard collimator, (B) restricted exit window and standard collimator, and (C) restricted exit window and modified collimator. By both restricting the exit window and using the modified collimator, leakage radiation outside of the intended treatment field is eliminated.

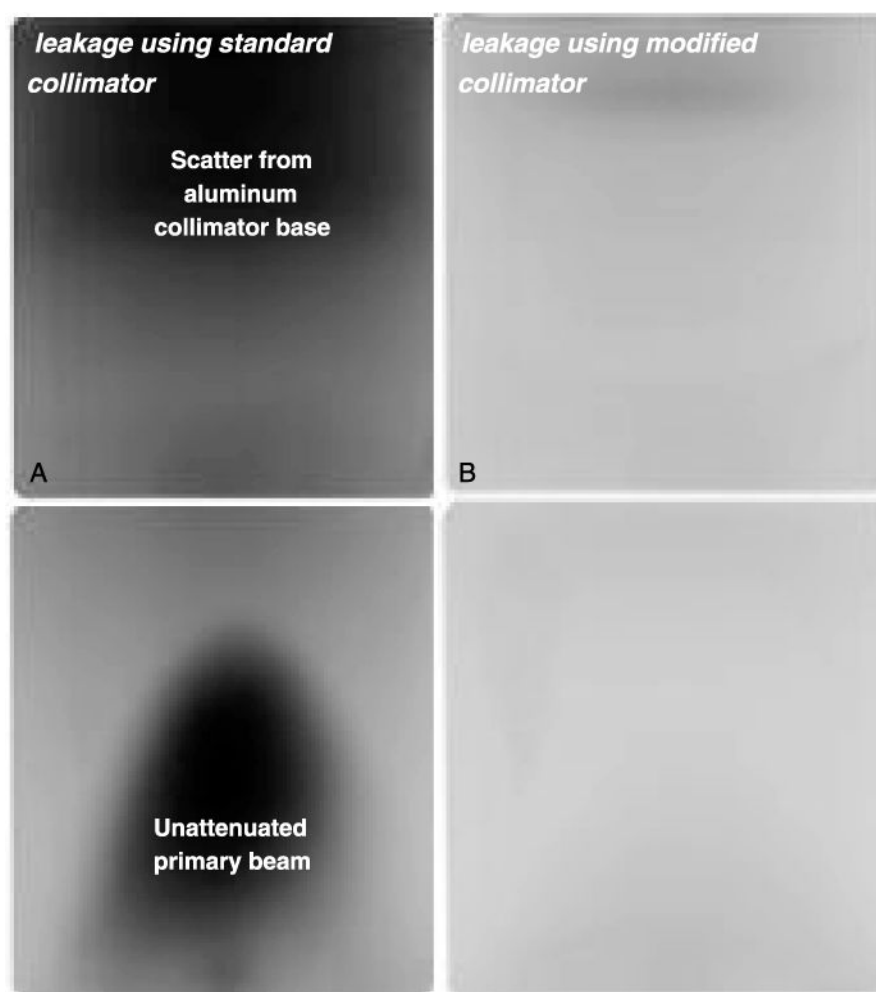


**Fig. 8.** XV films comparing exposure from (A) standard collimator and (B) modified collimator, in the plane of gantry rotation, 15 cm from the nozzle. The modified collimator reduces collimator scatter and completely blocks the primary beam outside the intended treatment field.

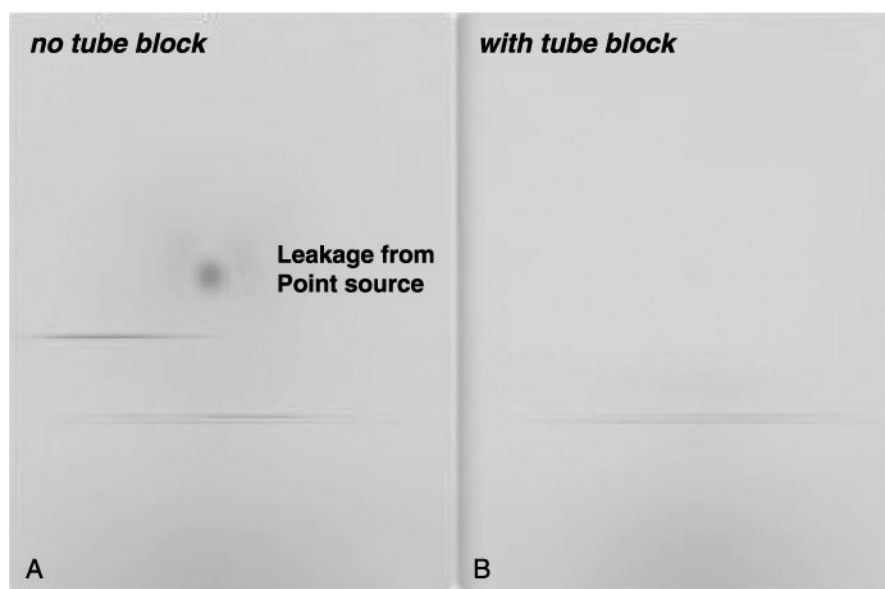


**Fig. 9.** XV films exposed directly in front of x-ray tube, comparing x-ray tube leakage (A) without and (B) with 3.2-mm-thick lead tube block. 3.2-mm-thick lead effectively blocks tube leakage.

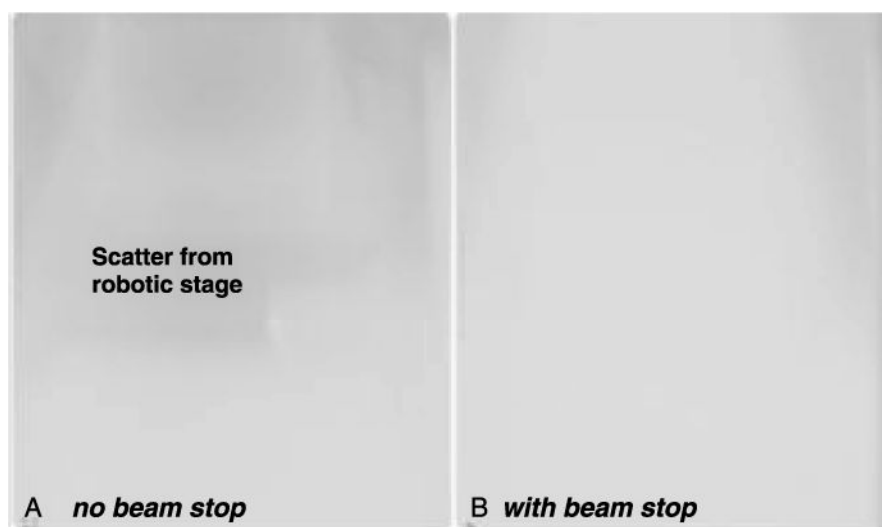


**Fig. 10.**  
XV films showing scatter from robot (A) without and (B) with lead beam stop.

**Table 1**

Effect of treatment energy on dose to bone.

kV	HVL (mm)	$E_{\text{eff}}$ (kV)	$\mu_{\text{en}}/\rho_{\text{water}}$ ( $\text{cm}^2 \text{g}^{-1}$ )	$\mu_{\text{en}}/\rho_{\text{bone}}$ ( $\text{cm}^2 \text{g}^{-1}$ )	$D_{\text{bone}}/D_{\text{water}}$
175	$0.45 \pm 0.03$	59	0.033	0.15	4.5
225	$0.58 \pm 0.04$	67	0.030	0.12	3.9

**Table 2**

Maximum percent of treatment dose received outside of treatment field, measured with EBT2 Gafchromic film at 35 cm SSD, 225 kV, 15 mA, 0.15 mm Cu filter.

Field size	Standard window, standard collimator	Restricted window, standard collimator	Restricted window, modified collimator
5 × 5 mm <sup>2</sup>	5.5%	0.4%	<0.2%
3 × 3 mm <sup>2</sup>	6.5%	0.4%	<0.2%
1 mm diameter	9.1%	0.5%	<0.2%

**Table 3**

Survey measurements outside enclosure before and after modifications to the collimator assembly 225 kV, 13 mA, 0.15 mm Cu filter,  $5 \times 5 \text{ mm}^2$  field size.

Location	Standard window, standard collimator ( $\mu\text{C kg}^{-1} \text{ h}^{-1}$ )	Restricted window, standard collimator ( $\mu\text{C kg}^{-1} \text{ h}^{-1}$ )	Restricted window, modified collimator ( $\mu\text{C kg}^{-1} \text{ h}^{-1}$ )
Outside glass window, height of isocenter	2.6	1.1	0.18
Top of glass window	7.7	3.6	0.52

**Table 4**

Survey measurements outside enclosure before and after shielding modifications 15 mm Cu filter, restricted exit window, modified collimator,  $5 \times 5 \text{ mm}^2$  field size.

Location	No modifications ( $\mu\text{C kg}^{-1} \text{ h}^{-1}$ )	3.2 mm Pb tube block, 225 kV, 13 mA ( $\mu\text{C kg}^{-1} \text{ h}^{-1}$ )	6.4 mm Pb beam stop, 225 kV, 13 mA ( $\mu\text{C kg}^{-1} \text{ h}^{-1}$ )	175 kV, 15 mA ( $\mu\text{C kg}^{-1} \text{ h}^{-1}$ )
Top of glass window	1.4	0.52	—	<0.03
Bottom of glass window	0.28	—	0.21	<0.03